

# 16

## Optical Coherence Tomography Findings in Vitreomacular Interface Disorders

Javier Elizalde, Santiago Abengoechea, and María F. de la Paz

Optical coherence tomography (OCT) images of the interface between the macula and vitreous are very well defined because of the difference in reflectivity of the relatively acellular vitreous and the parallel-fiber orientation of the inner retina.<sup>1</sup> Disorders such as epiretinal membranes (ERMs), vitreomacular traction syndrome (VMTS), and macular holes are readily imaged and recognized even by persons inexperienced in biomicroscopy. Optical coherence tomography has also significantly contributed to making an accurate differential diagnosis of all these entities and to better understanding the varying structural anomalies of the retina that can explain visual loss in highly myopic eyes. The information obtained from high-resolution evaluation of retinal anatomy in all these conditions also improves the clinician's ability to make the optimal treatment decision and provides an objective means to monitor disease progression and therapeutic response.

### Epiretinal Membrane

The ERM is known by many names in clinical and educational circles, including preretinal membrane, idiopathic preretinal macular gliosis, cellophane maculopathy, macular pucker, and surface wrinkling retinopathy.<sup>2</sup> The ERM represents an abnormal glial or fibrocellular proliferation on the surface of the retina, commonly located over the central fovea that can result in distortion of the macular architecture and the development of macular edema.<sup>1</sup> In early stages, epiretinal membrane may be asymptomatic, or it may create only a mild reduction in visual acuity. Its progression may cause metamorphopsia and lead to severe visual impairment. The ophthalmoscopic picture of this disorder ranges from a fine, glistening membrane overlying the macula (cellophane maculopathy) to a thickened, whitish tissue that obscures the underlying vasculature (Fig. 16.1).

As the epiretinal membrane progresses, traction at the level of the internal limiting membrane (ILM) creates a puckering effect. In this situation retinal folds radiating outward from

the macula might be seen (Fig. 16.2). Adjacent retinal vessels that course under the ILM often assume a “corkscrew” pattern, which is quite dramatic with fluorescein angiography. In very severe cases, macular edema and even retinal detachment have been known to occur (Fig. 16.3). Occasionally, ERMs can evolve into macular pseudoholes (Fig. 16.4), and ERMs are often seen in conjunction with either vitreomacular traction syndrome or idiopathic full-thickness macular holes.<sup>1,3</sup> More rarely, fibrocellular tissue growing from the ERM toward the vitreous cavity might also be seen.

Optical coherence tomography images of ERMs may be classified into two broad categories: globally adherent membranes and partially nonadherent membranes.<sup>3</sup> Both types of ERMs are usually visible on OCT images as a taut hyperreflective line contiguous with or anterior to the inner retinal surface.

Partially nonadherent ERMs are clearly visible on OCT images as they have sections of tissue that are separated from the anterior surface of the retina (Figs. 16.1 and 16.2). The ERM appears as a linear, thin, reflective band anterior to the retina with focal areas of attachment to the retinal surface. The appearance of such an ERM might be mimicked by a partially detached posterior vitreous surface. However, ERMs tend to be thicker and more reflective than the posterior vitreous. The reflection from an ERM may measure up to 60  $\mu\text{m}$  in thickness; this is rarely observed with a partially detached posterior vitreous.

Globally adherent ERMs are visible on OCT images as a contrast in reflectivity between the highly reflective ERM and the less reflective anterior surface of the retina. The adherence between the ERM and the anterior retina is uninterrupted in contrast to partially nonadherent ERMs (Fig. 16.5). Approximately 10% of globally adherent membranes detected clinically cannot be detected by OCT.<sup>1,3</sup> This is the result of difficulty, in some cases, in distinguishing the highly reflective ERM from the underlying reflective nerve fiber layer of the anterior retina. In these cases, the secondary effects of the membrane, such as loss of the normal foveal contour, variable

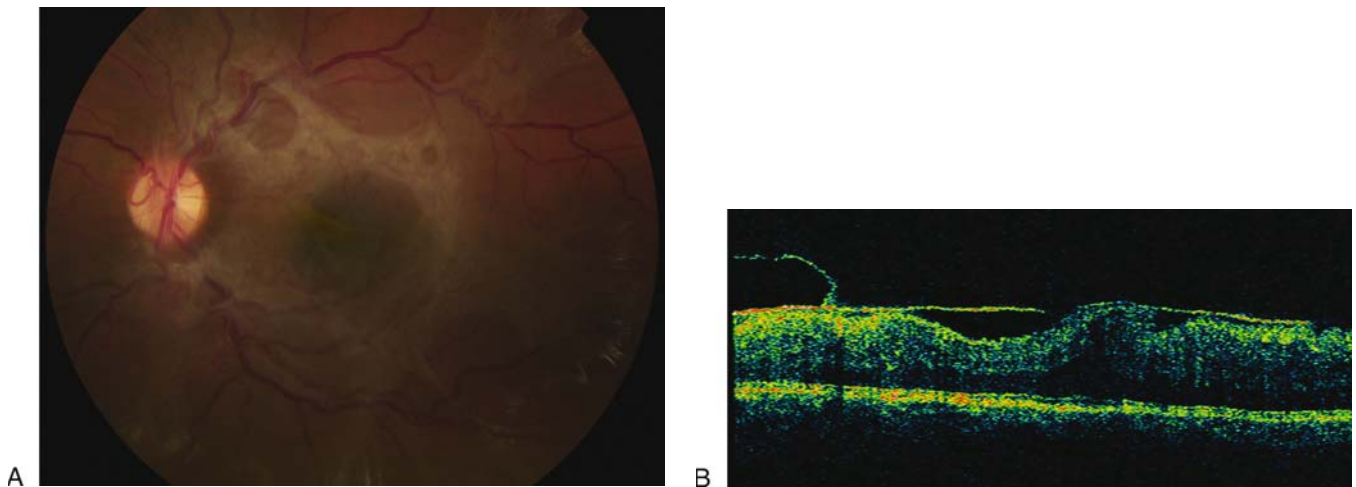


FIG. 16.1. A 37-year-old woman reports metamorphopsia in her left eye. Her visual acuity is 20/40 in this eye. (A) A dense star configuration of the central epiretinal membrane (ERM) was noted with foveal distortion (fold). Some vessels' segments are obscured by the membrane. (B) Optical coherence tomography (OCT) examination shows the ERM as a hyperreflective band with two focal well-defined points of attachment on the inner retinal surface and retinal thickening with folds. Note the correlation between the ophthalmoscopic appearance and the cross-sectional OCT image.

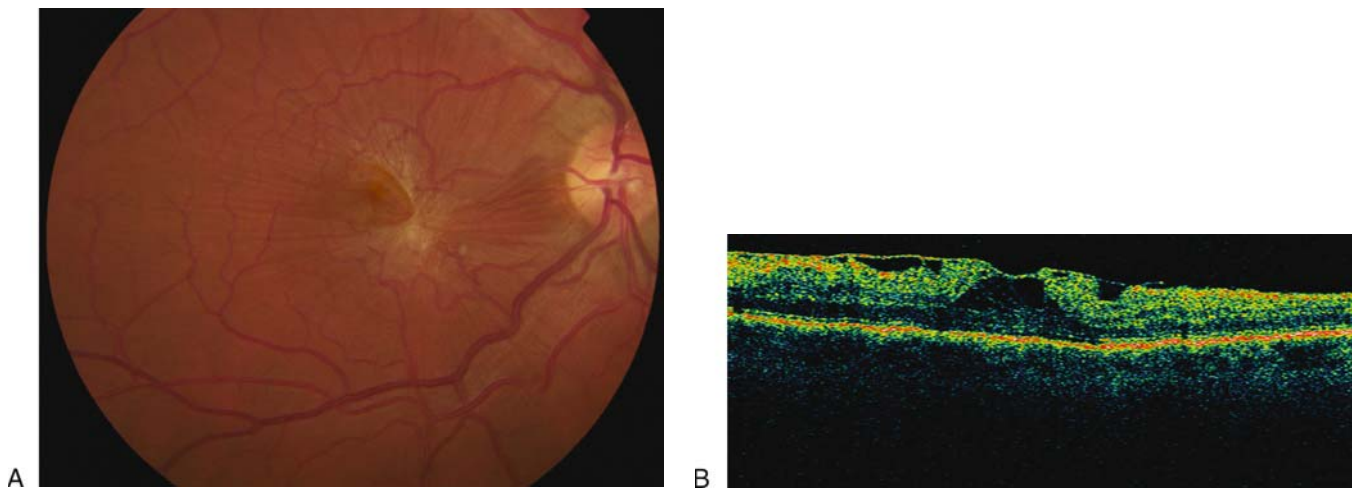


FIG. 16.2. (A) An ERM causing retinal folds radiating outward from the macula. (B) Optical coherence tomography reveals that the membrane is separated from the inner retina with multiple focal points of attachment.

irregularity of the inner retinal layers and macular thickening are used to establish the presence of the membrane.

In addition, characterization of the ERM with OCT may help in preoperative planning for membrane peeling.<sup>4</sup> In cases with separation between the membrane and retina, the surgeon may be directed to these areas to initiate membrane dissection. When the membrane is globally attached to the inner retina, the surgeon may anticipate more difficulty in peeling the membrane. The surgeon may also proceed with particular

caution when extensive intraretinal edema leaves a thin, friable inner retinal layer beneath the membrane.

Postoperative OCT imaging can be used to document surgical response (Fig. 16.5). The completeness of ERM removal can often be assessed by comparing preoperative and postoperative images. Usually retinal thickness decreases following successful ERM peeling,<sup>4,5</sup> visual acuity improves, and the distorted vascular pattern comes back to its normal morphology.

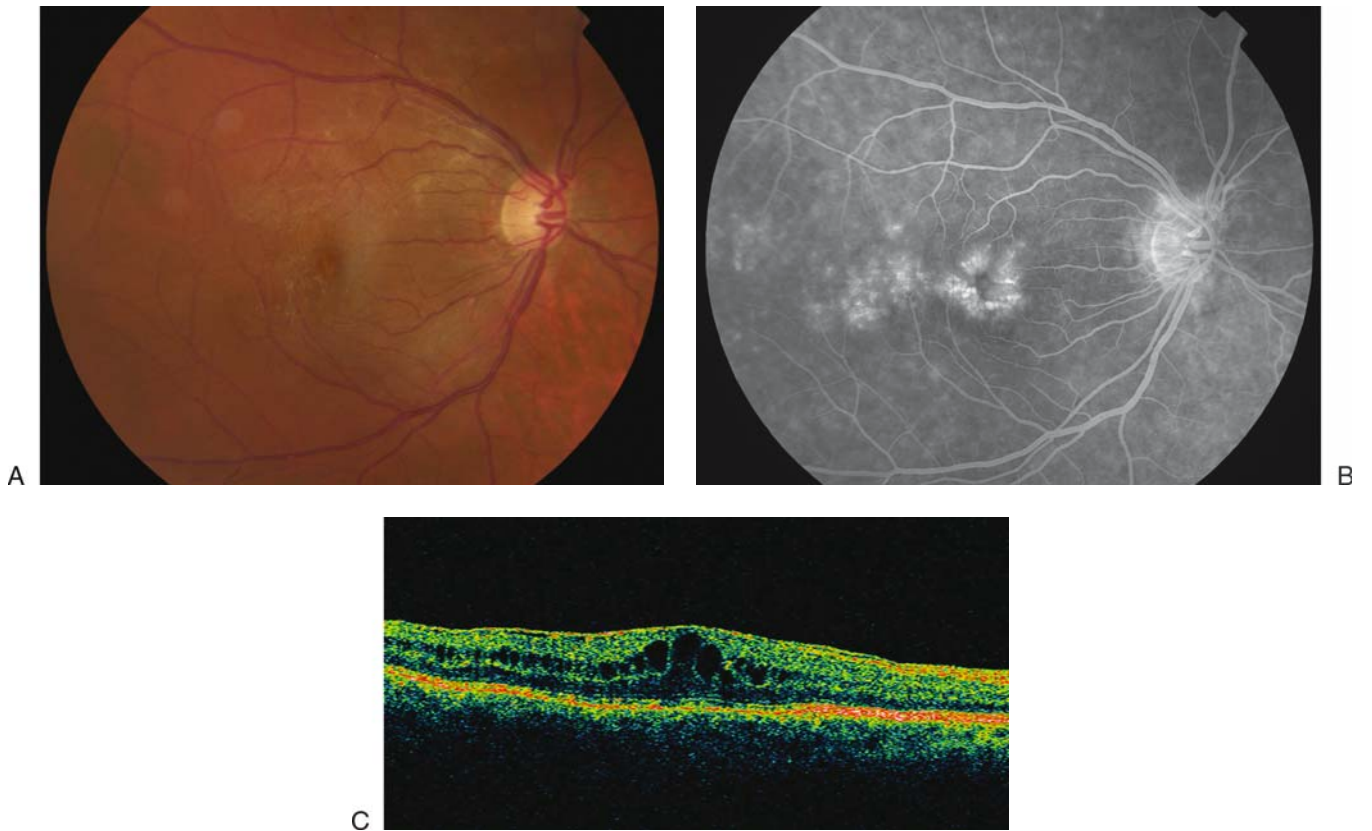


FIG. 16.3. (A) Bright reflex on the macula corresponding to an epiretinal proliferation. (B) Fluorescein angiography reveals late hyperfluorescence consistent with cystoid macular edema complicating this case. (C) Although the proliferation is globally adherent to the inner retina, the ERM can still be seen as a highly reflective band on the retinal surface. The fovea is extensively thickened from intraretinal edema with loss of the foveal depression and multiple intraretinal cysts are seen.

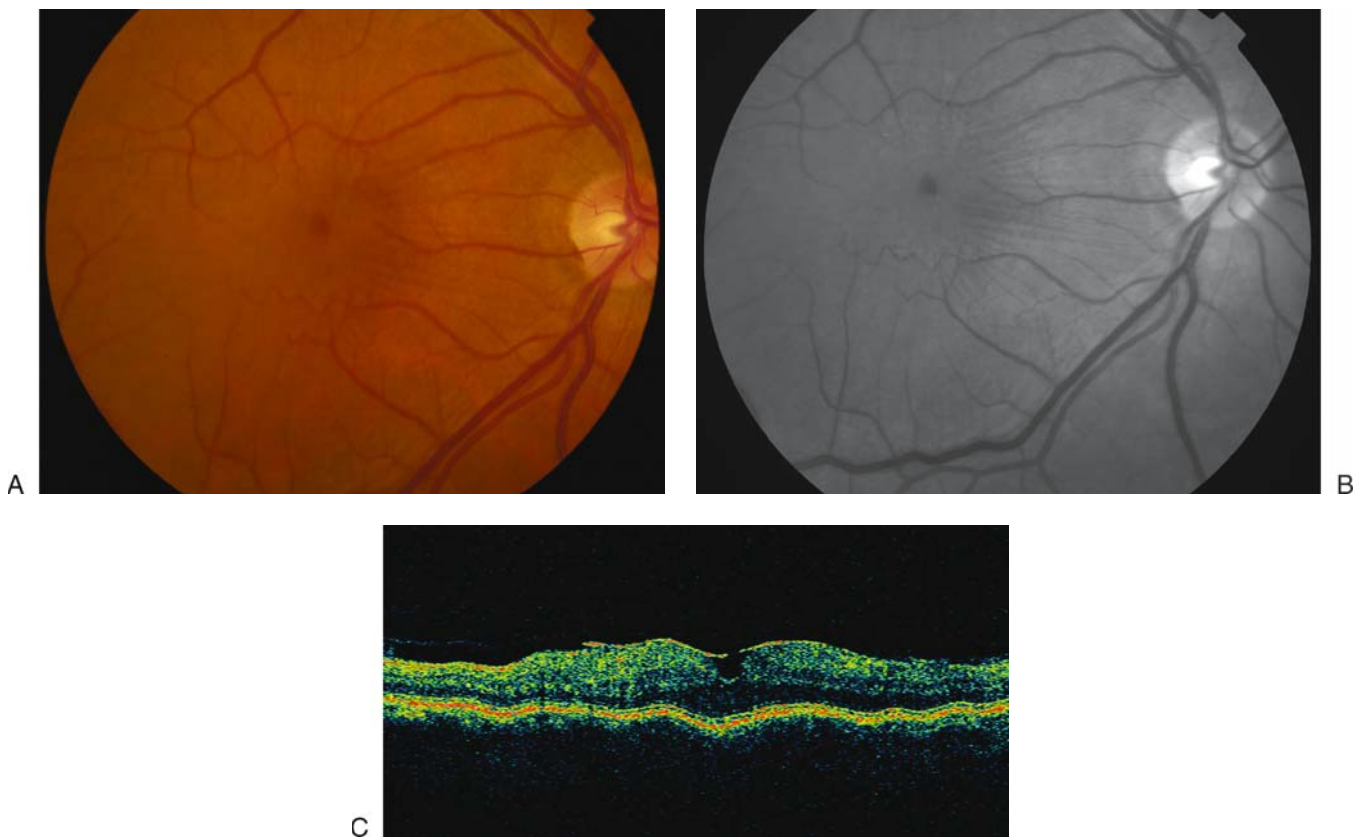


FIG. 16.4. (A-C) Epiretinal membrane and radial folds simulating a macular hole image (pseudomacular hole). (A) Color photograph. (B) Fluorescein angiography. (C) Optical coherence tomography.

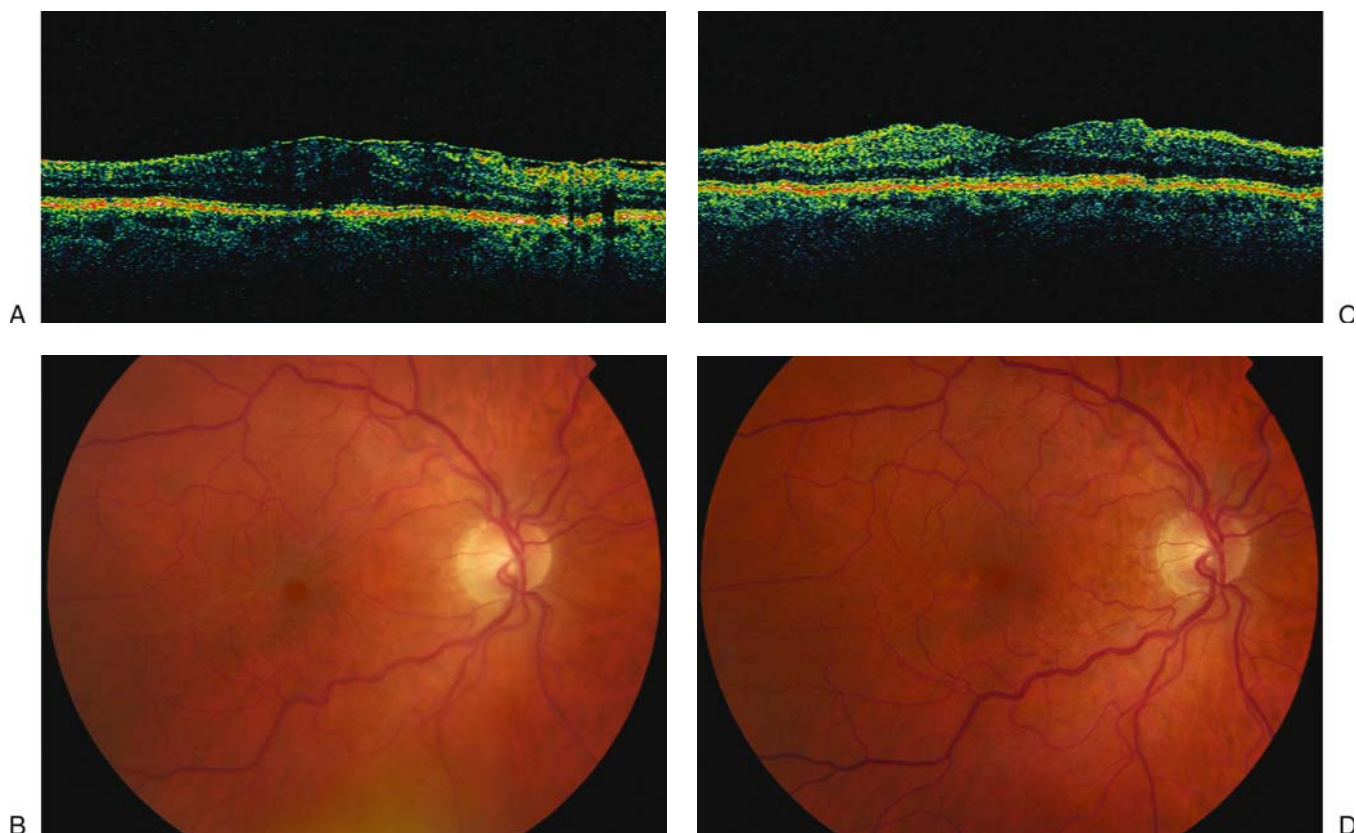


FIG. 16.5. Epiretinal membrane before (A,B) and after (C,D) surgical treatment. Postoperative OCT (C) demonstrates complete removal of the membrane, resulting in a normal foveal contour.

## Vitreomacular Traction Syndrome

Vitreomacular traction syndrome (VMTS) refers to conditions in which retinal changes develop from incomplete posterior vitreous detachment (PVD) with persistent vitreous adhesion to the macula. It differs from idiopathic ERM in that the posterior hyaloid, rather than being generally totally detached from the posterior retina surface, remains attached to the perifoveal region. It is also frequently attached at the optic nerve or at multiple other points along or inside the vascular arcades. Sometimes the vitreous adherence can be difficult or impossible to identify directly on clinical exam, yet will be obvious by OCT.<sup>6</sup> The VMTS membranes are frequently less reflective than ERMs and are associated with substantial foveal traction, intraretinal cystoid changes, cystoid macular edema (CME), and frank detachment of the fovea (Fig. 16.6). These changes result in central vision loss and metamorphopsia.

Although the vitreous attachment to the macula usually appears broad on clinical exam, OCT typically shows an incomplete V-shaped PVD temporally and nasally to the fovea but remaining attached to the fovea. This configuration appears identical to the vitreous attachment identified in idiopathic macular hole. Why some patients with these findings progress to CME (VMTS) while others develop macular holes

remains unclear. Variations in the location, density, and diameter of the vitreoretinal adhesion may explain these differences. Other VMTS cases can have a PVD temporally to the fovea but no posterior detachment nasally to it. In these cases prominent CME may develop, which may result in a macular hole or macular atrophy.<sup>7</sup>

As with other vitreoretinal interface abnormalities, OCT is extremely useful in monitoring the progression of patients with VMTS. Spontaneous resolution of vitreoretinal traction with normalization of the retinal contour has been documented with OCT.<sup>8,9</sup> On the other hand, persistent traction can lead to progressive retinal edema and thickening. Quantifying such changes with the OCT can be valuable in determining the need and timing of surgical intervention. As with ERMs, OCT can provide useful information in counseling the VMTS patient preoperatively with regard to visual potential. Eyes demonstrating massive traction, distortion of retinal architecture, intraretinal edema, and foveal detachment may be anticipated to have a relatively poor ultimate outcome compared to eyes not exhibiting these features. After surgery, OCT can be used to evaluate the anatomic response. Cases in the literature have documented improved retinal anatomy in association with increased visual acuity following vitrectomy surgery.<sup>10,11</sup>

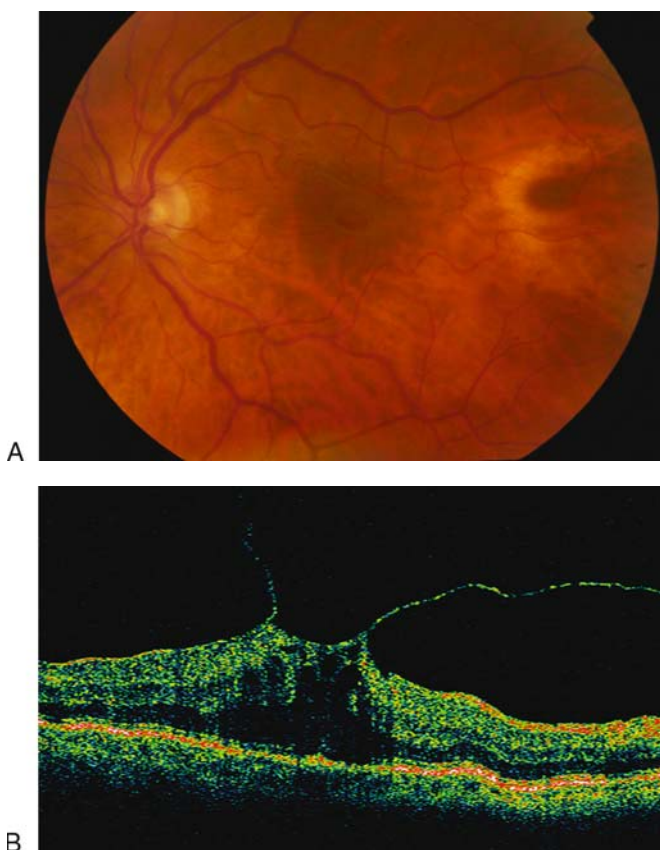


FIG. 16.6. A 58-year-old woman notes a progressive decrease in vision of the left eye over the past 6 months. (A) Fundus examination demonstrates a perifoveal ring-shaped fold with a glistening ERM. (B) Optical coherence tomography defines vitreomacular traction with attachment of the posterior hyaloid directly to the fovea. The tractional forces from the vitreous have resulted in retinal thickening with associated cystic spaces.

## Idiopathic Macular Hole

An idiopathic macular hole is a retinal defect in the foveal area. Its incidence is around 3 in 1000, and it is more common in women in the sixth and seventh decades of life.<sup>12,13</sup> The classification of idiopathic macular holes as proposed by Gass<sup>14,15</sup> has always been the standard in staging macular holes until the advent of the OCT. In stage 1, there is vitreomacular traction due to incomplete vitreous detachment, lifting the foveal area and the formation of an impending macular hole. This clinically appears as a yellowish spot on the fovea. As traction increases, the spot enlarges to form a yellowish cyst (stages 1a and 1b). In stage 2, Gass describes a break in the retinal contour while the operculum is still attached to the retina, or separated from the underlying retina but with a hole diameter of less than 400  $\mu\text{m}$ . In stage 3, there is complete separation of the operculum from the underlying retina, with a hole diameter more than 400  $\mu\text{m}$ . In stage 4, there is complete posterior vitreous detachment with release of the anteroposterior tractional forces.

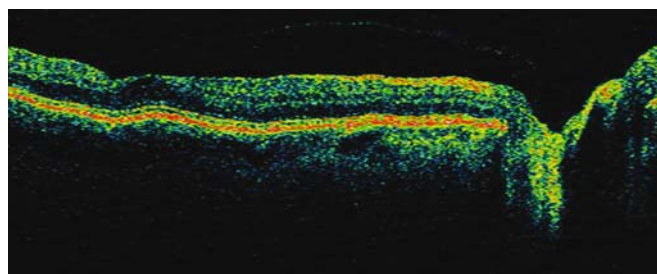


FIG. 16.7. Stage 1A macular hole. Vitreomacular traction with partial-thickness foveal pseudocyst. Papillomacular axis.

Since the introduction of the OCT, staging of macular holes has changed, especially with respect to the early stages. Gaudric et al.<sup>16</sup> described stage 1 as the presence of a cystic retinal space without foveal detachment similar to the clinical description of Gass. The authors proposed that this space was brought about by the anteroposterior traction from the posterior hyaloid, causing damage to central structures of the cellular processes of Müller cells. Optical coherence tomography imaging shows a hyporeflective space in the inner third of the fovea, along with loss of the normal foveal contour and a hyperreflective band adherent to the inner retina (posterior hyaloid). The early detection of stage 1 idiopathic macular holes was made possible by doing OCT imaging of the contralateral eye of those with already diagnosed macular holes.

The initial finding is an incomplete detachment of the posterior hyaloid around the fovea with no changes in the underlying retina. This is probably because of the existing vitreofoveal adhesion. The presence of a tight bond of the posterior hyaloid over the fovea and the optic nerve head gives rise to vitreomacular traction. There is no consensus as to how the foveal cyst or pseudocyst evolves into a full-thickness macular hole. However, some authors, such as Gaudric et al., believe that a full-thickness macular hole proceeds from a break in the inner retinal surface caused by the existing tractional forces. Some consider that the foveal cystic space burrows deep until the photoreceptor layer prior to the breaking of the inner retinal wall.<sup>15</sup> Altaweel and Ip<sup>17</sup> published the latest staging of idiopathic macular holes based on OCT findings:

- Stage 1A: Pseudocysts form (hyporeflective image on OCT) without affecting all retinal layers and with an intact outer retina (Figs. 16.7 and 16.8).
- Stage 1B: The foveal pseudocyst affects all retinal layers including photoreceptor layer and with intact roof. There is incomplete posterior vitreous detachment with persistent adhesion onto the fovea in stages 1A and 1B.
- Stage 2A: A break in the roof of the pseudocyst gives rise to a full-thickness macular hole. There is persistent traction of the posterior hyaloid that is firmly attached to the inner retina (Fig. 16.9).
- Stage 2B: Appearance of a retinal operculum is due to complete detachment of the posterior hyaloid from the inner retina. At this point, there is release of the anteroposterior

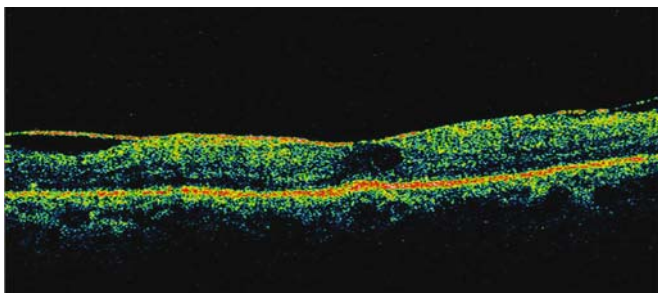


FIG. 16.8. Stage 1A macular hole. Foveal pseudocyst with intact photoreceptor layer and vitreomacular traction.

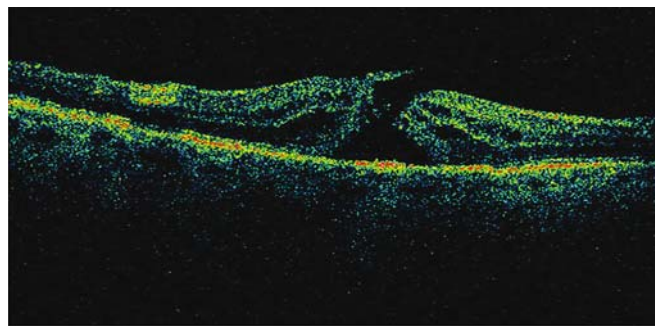


FIG. 16.9. Stage 2A macular hole. Vitreomacular traction (focal vitreous attachment to flap) with break in the roof of the foveal cyst.

tractional forces. The distance between the edges of the hole is less than 400  $\mu\text{m}$  (Fig. 16.10).

- Stage 3: The prefoveal operculum can still be appreciated but the distance between the hole edges is greater than 400  $\mu\text{m}$ . The posterior hyaloid is completely detached from the inner retina as opposed to the description of Gass wherein the former remains attached to the perifoveal area (Fig. 16.11).
- Stage 4: Complete detachment of the vitreous occurs, which cannot be seen tomographically and can only be confirmed by slit-lamp biomicroscopy or ultrasonography (Fig. 16.12).

Therefore, the main differences between the biomicroscopic and the OCT staging of idiopathic macular holes are the presence of a tight focal foveolar adherence of the posterior hyaloid versus a perifoveal vitreomacular detachment, the formation of a foveal pseudocyst versus a detachment in Gass's stage 1 hole, and the subdivision of stage 2 into two distinct anatomical types.

Optical coherence tomography is likewise useful in assessing the prognosis of an idiopathic macular hole. In the study of Gaudric et al.<sup>16</sup> in which 76 contralateral eyes were

studied using OCT, the authors found the presence of intraretinal changes or traction in 15 eyes. Considering that the probability of developing a macular hole in the contralateral eye is 13% in 48 months,<sup>18</sup> it is then mandatory to perform bilateral tomographic imaging in patients affected by this pathology for early detection in the other eye. In another study of 66 contralateral asymptomatic eyes, the authors concluded that the presence of a foveal cyst connotes a 55% risk of developing a full-thickness macular hole in asymptomatic eyes, and that vitreofoveal separation signifies good prognosis.<sup>19</sup> Moreover, it has been shown that the smaller the diameter of the macular hole preoperatively, the higher the probability of anatomic closure. In those cases with a base diameter less than 400  $\mu\text{m}$  as measured by OCT, an anatomic closure was achieved in 92%, and in those with a base diameter more than 400  $\mu\text{m}$ , this value decreased to 56%.<sup>20</sup>

Several variables, such as preoperative visual acuity, duration of symptoms, OCT measurement of hole diameter (as a single variable), and stereoscopic funduscopy, may predict the final visual outcome.<sup>21</sup> One study demonstrated that the

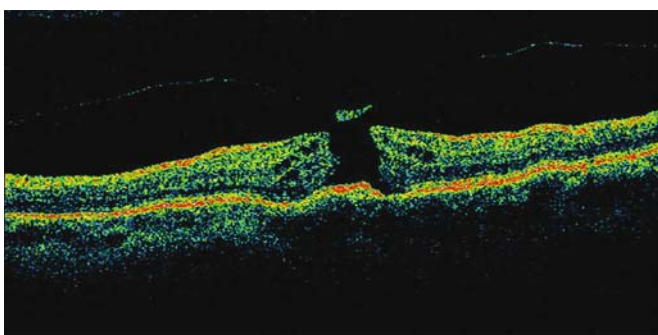


FIG. 16.10. Stage 2B macular hole. Preretinal operculum with distance between hole edges less than 400  $\mu\text{m}$ . Microcystic spaces are seen at the edges of the hole.

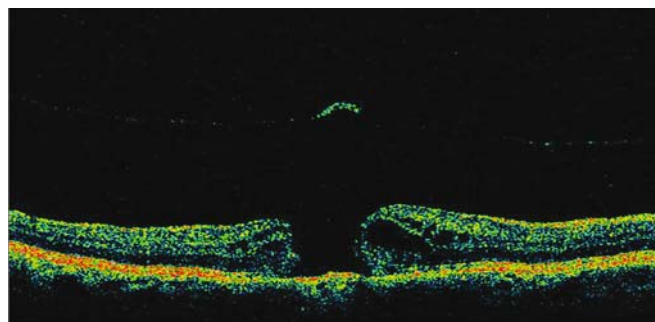


FIG. 16.11. Stage 3 macular hole. Preretinal operculum with distance between hole edges greater than 400  $\mu\text{m}$ . Cystic degeneration of the borders of the hole is more evident.

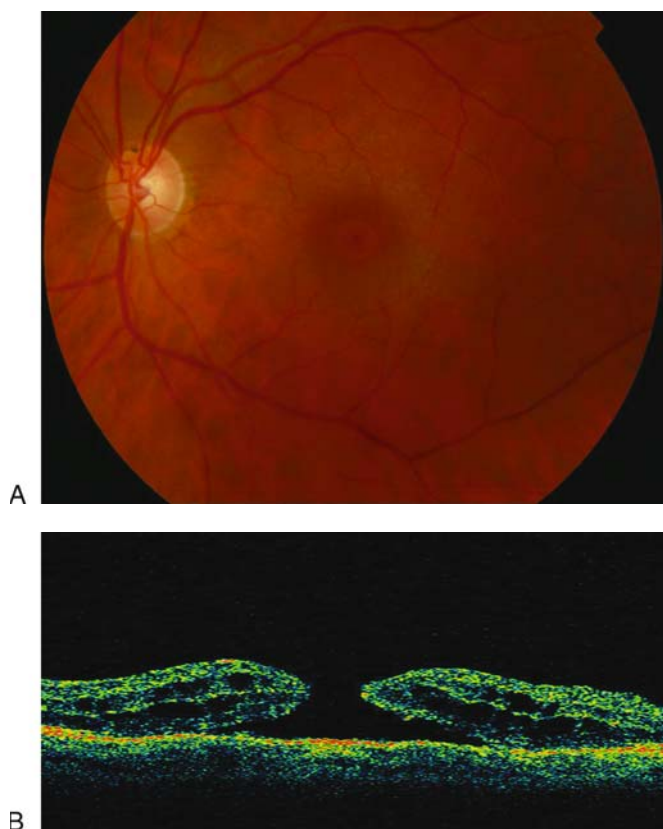


FIG. 16.12. (A) Biomicroscopic image of a full-thickness macular hole. (B) Stage 4 macular hole. Big intraretinal cysts are seen with lifting of the borders. No vitreomacular traction is noted.

OCT measurement is predictive not only of the possibility of anatomic closure but also of postoperative visual acuity. By using the maximum hole diameter, minimum hole diameter and height as reference values, the authors use a formula to infer macular hole prognosis.<sup>22</sup>

Optical coherence tomography is likewise useful in evaluating anatomic closure after macular hole surgery. The flattening of the retina and the disappearance of the retinal cysts may be appreciated postoperatively. The closure of the horizontal component of a hole wherein there is complete detachment usually takes place in the first postoperative month. Absence of closure within the first postoperative month entails a poor prognosis.<sup>23</sup> In the normal course of an idiopathic macular hole, about 2% may close by themselves spontaneously when there is release of vitreomacular traction (Fig. 16.13). In such cases, the photoreceptors may be affected due to the previously existing traction, and, as a consequence, may give rise to an absolute central scotoma. The differential diagnosis of macular pseudoholes and lamellar holes is discussed in the following chapter on myopic tractional maculopathy.

Thus, OCT imaging is a highly important tool in the diagnosis, in the evaluation of the etiopathogenesis, in the postoperative follow-up, and as a predictive factor in the prognosis of idiopathic macular holes.

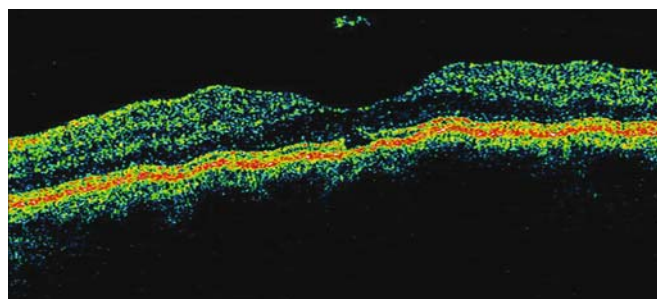


FIG. 16.13. Spontaneous closure of a macular hole with a preretinal operculum and central defect in the photoreceptor layer.

## Myopic Tractional Maculopathy

High myopia is defined as an elongation of the anteroposterior axis of the globe associated with an axial length greater  $\geq 26$  mm. This pathology causes a progressive weakening of the scleral wall and axial elongation, which in severe cases may give rise to a posterior staphyloma. A posterior staphyloma may cause lesions such as chorioretinal atrophy, focal breaks in Bruch's membrane (lacquer cracks), subretinal hemorrhages, and chorioretinal neovascular membranes entailing very poor visual outcome. High myopia is known to have a prevalence of about 2% in the general population and about 22% to 33% in myopic eyes.<sup>24</sup> This clinical entity is usually bilateral, affecting patients of working age, and may produce an average legal blindness duration of 17 years.<sup>25</sup>

Optical coherence tomography enables us to capture high-resolution images of the posterior pole. This imaging technique is highly useful in examining the vitreomacular interface. Moreover, it enables precise characterization of the lesions that previously could only be appreciated on histologic sections. For example, with OCT, we can now distinguish between a retinoschisis and a flat retinal detachment at the macular area. The imaging protocol that we use for myopic tractional maculopathy consists of six sections, each 6 mm long centered on the fovea, a section along the optic nerve linking with the macula and six parallel sections connecting the temporal vascular arcades. With the said imaging protocol, we can scan the entire macula and visualize the presence or absence of traction, and the possible consequences on the fovea.

Myopic tractional maculopathy encompasses several lesions such as macular thickening, retinoschisis, lamellar holes, and retinal detachment due to tractional phenomena in patients with high myopia. Traction may be tangential or anteroposterior. Takano and Kishi<sup>26</sup> were the first ones to describe this clinical entity using OCT. Slit-lamp examination of these patients using a standard 60, 78, or 90 diopter lens is usually normal and neither traction nor retinal detachment can be appreciated. In some cases, we may find a microcystic appearance in the area of the posterior staphyloma that could make us suspect a possible tractional maculopathy. Rochon-Duvigneaud<sup>27</sup> was

the first one to describe the biomicroscopic findings of this pathology, but it was not until the advent of OCT that its characteristics were described in full detail. Green<sup>28</sup> described the presence of schisis in the peripheral retina in histopathologic studies but was not able to demonstrate where the traction came from. He related that these lesions were brought about by the lack of elasticity of some retinal components, especially the retinal vessels and the internal limiting membrane, in the light of an already weakened scleral wall and progressive elongation of the globe.

The first OCT finding in these patients is a thickening of the macular area along with loss of the normal foveal contour. In these cases, we should perform a scan of the macular area to find out what is causing this retinal thickening. Nonetheless, it may take years for this clinical process to evolve until such time that the patient may note some visual symptoms.

Another characteristic finding of myopic tractional maculopathy is the presence of a hyporeflective space dividing the sensorineural retina into two layers. The first is a fine layer of moderate reflectivity in apposition to the retinal pigment epithelium, and the second is a thicker hyperreflective layer in the inner retina. In this wide hyporeflective space, we may find some strands uniting the inner and the outer retina. The tomographic patterns of myopic retinal schisis may vary. The internal fibers may take on a “V” pattern and delineate the central cyst, or it may demarcate the boundary of a lamellar hole (superior opening of the cyst) or it may be associated with a foveal retinal detachment (Figs. 16.14 to 16.17). Nevertheless, when there is some degree of detachment in the internal retina, it may be called retinoschisis of the inner layers.

Other tomographic findings of myopic tractional maculopathy include retinal detachment. These are hyporeflective areas apposed to the retinal pigment epithelium with well-defined borders. They are usually located in the foveal area and associated with retinoschisis of the outer layers. Benhamou et al.<sup>29</sup> suggested that this finding may be a precursor of the myopic macular hole. Most cases would show that the widest area of detachment coincides with the peak of the vitreomacular traction (Fig. 16.16). Lamellar macular holes may likewise be found in these tractional phenomena (Fig. 16.18). However, the tomographic image is different from an idiopathic macular pseudohole (Fig. 16.19). The latter presents with an epiretinal membrane and is firmly adherent to the inner retinal surface. The edges of a pseudohole form a straight angle, while those of a lamellar hole form a more open angle. In most cases, the lamellar holes are brought about by a break in the roof of a retinal cyst (Fig. 16.20), but in myopic tractional maculopathy we may find some traction in the edges of the retinal hole. There are different anomalies existing in the vitreomacular interface that bring about this clinical entity. There may be anteroposterior forces such as vitreomacular traction wherein there is a perifoveal vitreous detachment with focal adhesion to the macula. Likewise, there may be tangential forces such as in the case of an epiretinal membrane where various points of traction may be found. Sometimes it may be difficult to determine the

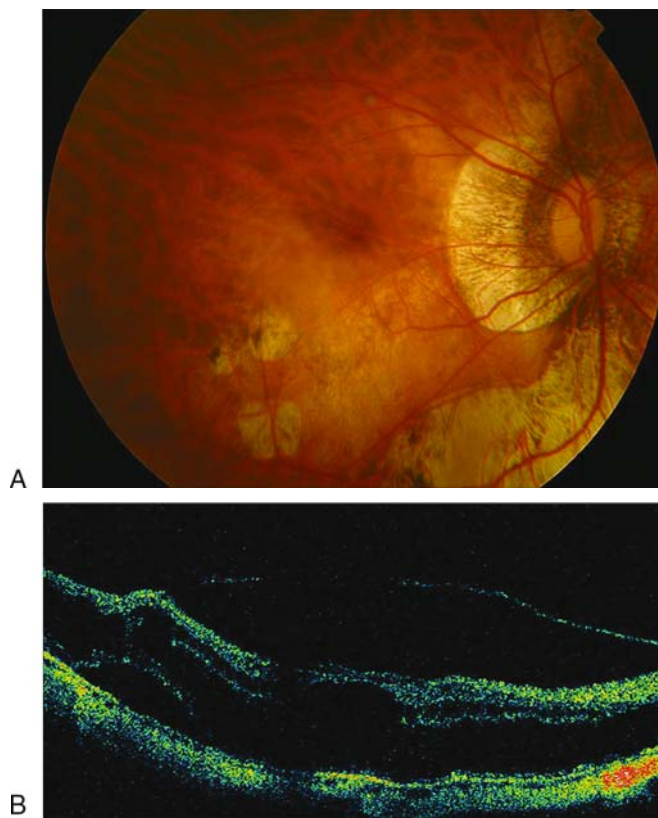


FIG. 16.14. (A) Myopic fundus with posterior staphyloma. (B) Retinoschisis of the outer retinal layers with foveal cyst and tractional retinal detachment.

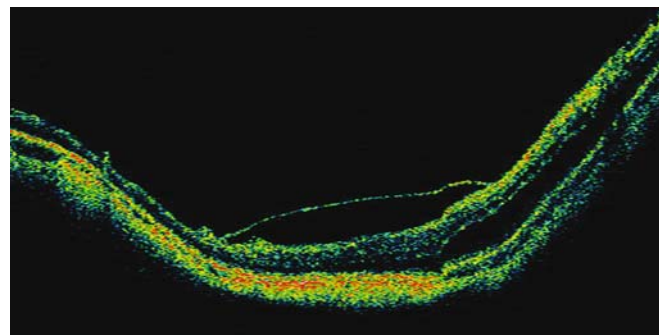
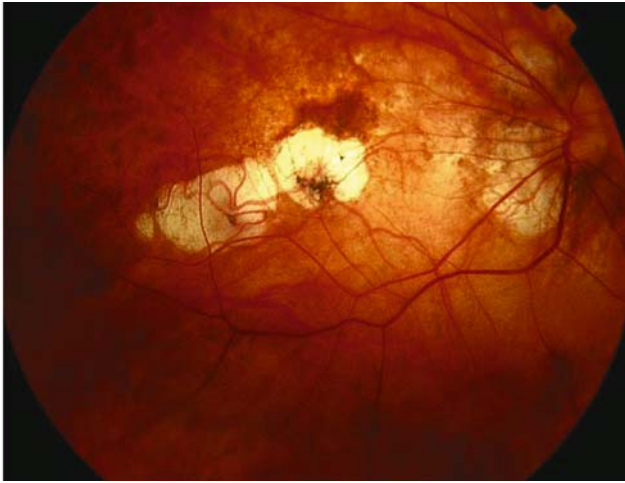


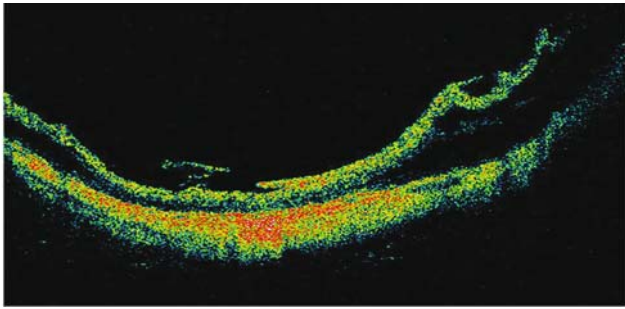
FIG. 16.15. Vitreomacular traction with retinoschisis of outer layers. Note the posterior staphyloma.

principal cause of the traction since the lesions and the tomographic images of the said entities are very similar. Moreover, a combination of both mechanisms may exist. There may be anteroposterior traction, tangential traction, incomplete posterior vitreous detachment, and an epiretinal membrane.

Another mechanism that must not be overlooked is the presence of an external traction brought about by the inherently weakened scleral walls and the posterior staphyloma. The said external tractional forces heightens the internal tractional forces similar to what occurs in non-high myopes who have epiretinal



A



B

FIG. 16.16. (A) Retinography of a high myopic eye without evidence of vitreomacular traction. (B) Retinoschisis of the outer layers with peaking of vitreomacular traction in the form of a tent.

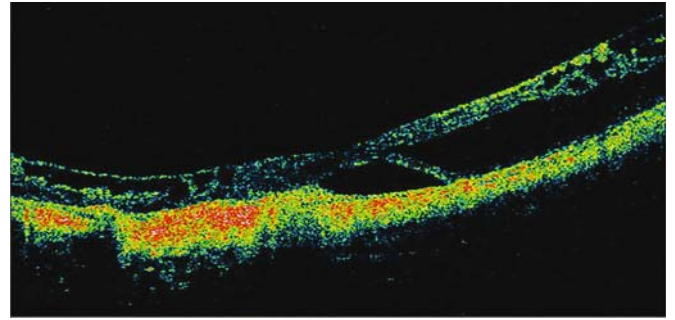


FIG. 16.17. Retinoschisis of the outer layers, inner layers, and dome-shaped retinal detachment.

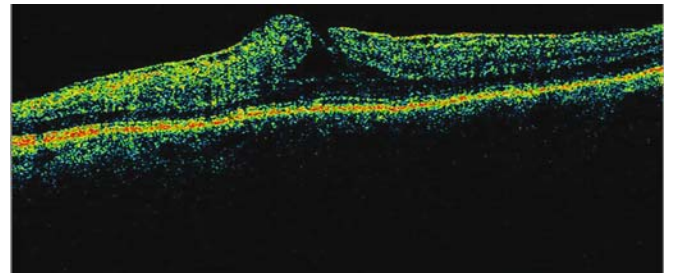
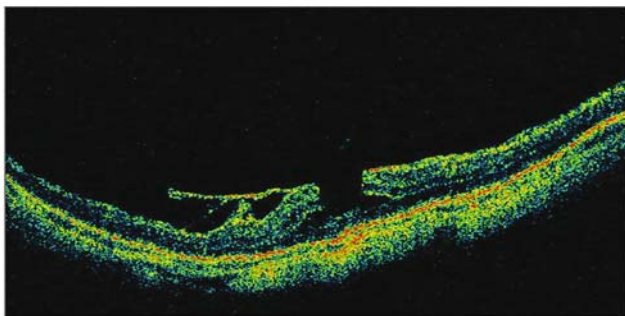


FIG. 16.19. Macular pseudohole with an internal hyperreflective band corresponding to an epiretinal membrane.



A



B

FIG. 16.18. (A) Myopic fundus with macular pigmented epithelium atrophy. (B) Lamellar hole with vitreomacular traction. Note the opened angle and the elevation of the hole's border.

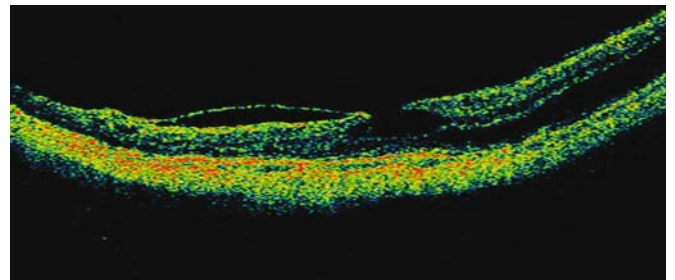


FIG. 16.20. Lamellar hole without vitreomacular traction in a non-myopic patient.

Table 16.1. Summary of results from 125 myopic eyes focusing on traction and retinal damage.

	No. of eyes (%)
Sample size	125
Epiretinal traction	58 (46.4)
•Epiretinal membrane	31 (24.8)
•Vitreomacular traction	11 (8.8)
•Epiretinal membrane + vitreomacular traction	16 (12.8)
Consequent retinal lesions	43 (34.4)
•Macular retinoschisis	25 (20.0)
•Retinal thickening	10 (8.0)
•Lamellar hole	6 (4.8)
•Retinal detachment	2 (1.6)
Staphyloma	53 (42.4)

Source: Adapted from Panozzo and Mercanti.<sup>30</sup>

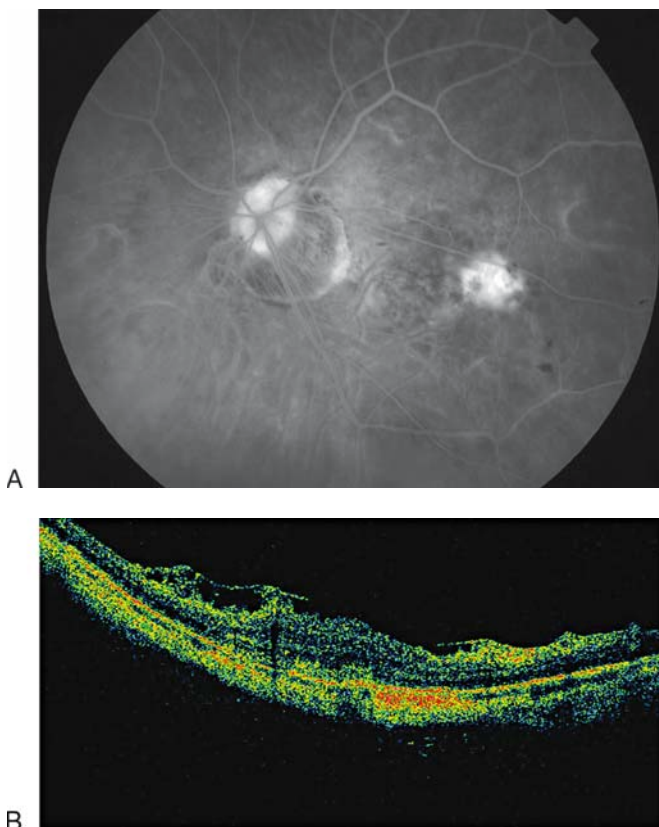


FIG. 16.21. (A) Central hyperfluorescence area corresponding to a subretinal neovascular membrane in high myopia. (B) Neovascular membrane over the retinal pigment epithelium with associated macular edema and preretinal tractional phenomena.

membranes and vitreomacular traction. Panozzo and Mercanti<sup>30</sup> reported the lesions encountered in 125 eyes with high myopia and the corresponding causes of the said lesions (Table 16.1).

The existing tractional forces in the macular area may likewise be associated with other lesions such as subretinal neovascularization. In such cases, imaging with OCT is useful to demonstrate the tractional forces that a simple fluorescein/indocyanine angiography would not reveal (Fig. 16.21).

At present, there is no consensus about the proper term of this clinical entity. Some authors refer to the OCT image of the lesions and label them as myopic macular retinoschisis<sup>28</sup> or myopic macular foveoschisis.<sup>31</sup> We consider it more appropriate to refer to the encompassing origin of these retinal lesions and call this clinical entity “myopic tractional maculopathy” as Panozzo and Mercanti<sup>30</sup> introduced the term recently.

## References

1. Voo I, Mavofrides EC, Puliafito C. Clinical applications of optical coherence tomography for the diagnosis and management of macular diseases. *Ophthalmol Clin North Am* 2004;17:21–31.
2. Gass JDM. Macular dysfunction caused by vitreous and vitreoretinal interface abnormalities. Vitreous traction maculopathies. In: Gass JDM (Ed.). *Stereoscopic Atlas of Macular Diseases*. St Louis: Mosby, 1987.
3. Wilkins JR, Puliafito CA, Hee MR, et al. Characterization of epiretinal membranes using optical coherence tomography. *Ophthalmology* 1996;103:2142–2151.
4. Massin P, Allouch C, Haouchine B, et al. Optical coherence tomography of idiopathic epiretinal membranes before and after surgery. *Am J Ophthalmol* 2000;130:732–739.
5. Gallemore RP, Jumper JM, McCuen BW, et al. Diagnosis of vitreoretinal adhesions in macular disease with optical coherence tomography. *Retina* 2000;20:115–120.
6. Smiddy WE, Michels RG, Glaser BM, De Bustros S. Vitrectomy for macular traction caused by incomplete vitreous separation. *Arch Ophthalmol* 1988;106:624–628.
7. Yamada N, Kishi S. Tomographic features and surgical outcomes of vitreomacular traction syndrome. *Am J Ophthalmol* 2005;139:112–117.
8. Sulkes DJ, Ip MS, Baurnal CR, Wu HK, Puliafito CA. Spontaneous resolution of vitreomacular traction documented by optical coherence tomography. *Arch Ophthalmol* 2000;118:286–287.
9. Kusaka S, Saito Y, Okada AA, et al. Optical coherence tomography in spontaneously resolving vitreomacular traction syndrome. *Ophthalmologica* 2001;215:139–141.
10. Munuera JM, García-Layana A, Maldonado MJ, et al. Optical coherence tomography of successful surgery of vitreomacular traction syndrome. *Arch Ophthalmol* 1998;116:1388–1389.
11. Uchino E, Uemura A, Doi N, Ohba N. Postsurgical evaluation of idiopathic vitreomacular traction syndrome by optical coherence tomography. *Am J Ophthalmol* 2001;132:122–123.
12. Ho AC, Guyer DR, Fine SL. Macular hole. *Surv Ophthalmol* 1998;42:393–416.
13. Chew EY, Sperduto RD, Hiller R, et al. The eye diseases case-control study. Clinical course of macular holes. *Arch Ophthalmol* 1999;117:242–246.
14. Gass JDM. Idiopathic senile macular holes: its early stages and pathogenesis. *Arch Ophthalmol* 1988;106:629–639.
15. Gass JDM. Reappraisal of biomicroscopic classification of stages of development of a macular hole. *Am J Ophthalmol* 1995;119:752–759.
16. Gaudric A, Haouchine B, Massin P, Paques M, Blain P, Erginay A. Macular hole formation: new data provided by optical coherence tomography. *Arch Ophthalmol* 1999;117:744–751.

17. Altaweel M, Ip M. Macular hole: improved understanding of pathogenesis, staging, and management based on optical coherence tomography. *Semin Ophthalmol* 2003;18(2):58–66.
18. Lewis MI, Cohen SM, Smiddy WE, Gass JD. Bilaterality of idiopathic macular holes. *Graefes Arch Clin Exp Ophthalmol* 1996;234:241–245.
19. Spiritus A, Dralands L, Stalmans P, Stalmans I, Spileers W. OCT study of fellow eyes of macular holes. *Bull Soc Belge Ophthalmol* 2000;275:81–84.
20. Ip M, Baker BJ, Duker JS, et al. Anatomical outcomes of surgery for idiopathic macular hole as determined by optical coherence tomography. *Arch Ophthalmol* 2002;120(1):29–35.
21. Tilanus MAD, Cuupyers MHM, Bemelmans NAM, et al. Predictive value of pattern VEP, pattern ERG and hole size in macular hole surgery. *Graefes Arch Clin Exp Ophthalmol* 1999;237:629–635.
22. Ullrich S, Haritoglou C, Gass C, Schaumberger M, Ulbig MW, Kampik A. Macular hole size as a prognostic factor in macular hole surgery. *Br J Ophthalmol* 2002;86(4):390–393.
23. Jumper M, Gallemore R, McCuen BW, Toth CA. Features of macular hole closure in the early postoperative period using optical coherence tomography. *Retina* 2000;20:232–237.
24. Mondon H. Physiopathologie de la myopie forte. In: Mondon H, Metge P, eds. *La Myopie Forte*. Paris: Masson, 1994:29–57.
25. Green JS, Bear JC, Johnson GJ. The burden of genetically determined eye disease. *Br J Ophthalmol* 1986;70:696–699.
26. Takano M, Kishi S. Foveal retinoschisis and retinal detachment in severely myopic eyes with posterior staphyloma. *Am J Ophthalmol* 1999;128:472–476.
27. Rochon-Duvigneaud M. Déformation et lésions de l'œil myope. In: Mawas J, ed. *Introduction à L'étude de la myopie et des chorio-rétinites myopiques*. Bull Soc Ophthalmol Paris 1938;1:1–10.
28. Green WR. Retina, myopia. In: Spencer WH ed. *Ophthalmic Pathology: An Atlas and Textbook*, vol 2, 4th ed. Philadelphia: WB Saunders, 1996:913–924.
29. Benhamou N, Massin P, Haouchine B, Erginay A, Gaudric A. Macular retinoschisis in highly myopic eyes. *Am J Ophthalmol* 2002;133:794–800.
30. Panozzo G, Mercanti A. Optical coherence tomography findings in myopic traction maculopathy. *Arch Ophthalmol* 2004;122:1455–1460.
31. Ikuno Y, Sayanagi K, Ohji M, et al. Vitrectomy and internal limiting membrane peeling for myopic foveoschisis. *Am J Ophthalmol* 2004;137:719–724.